Shock Metamorphism of the Coconino Sandstone at Meteor Crater, Arizona[1]

Susan Werner Kieffer[2]

Division of Geological and Planetary Sciences
*California Institute of Technology, Pasadena 91109*

A study of the shocked Coconino sandstone from Meteor Crater, Arizona, was undertaken to examine the role of porosity in the compression of rocks and in the formation of high-pressure phases. A suite of shocked Coconino specimens collected at the crater is divided into five classes, arranged in order of decreasing quartz content. The amounts of coesite, stishovite (measured by quantitative X-ray diffraction), and glass vary systematically with decreasing quartz content. Coesite may comprise ⅓ by weight of some rocks, whereas the stishovite content does not exceed 1%. The five classes of rocks have distinct petrographic properties, correlated with the presence of regions containing coesite, stishovite, or fused silica. Very few occurrences of diaplectic glass are observed. In the lowest stages of shock metamorphism (class 1), the quartz grains are fractured, and the voids in the rock are filled with myriads of small chips derived from neighboring grains. The fracture patterns in the individual quartz grains are controlled by the details of the initial morphology of the colliding grains. In one weakly shocked rock, it was possible to map the general direction of shock passage by recording the apparent direction of collision of individual grains. The principal mechanism of energy deposition by a shock wave in a porous material is the reverberation of shock and rarefaction waves through grains due to collisions with other grains. A one-dimensional model of the impact process can predict the average pressure, volume, and temperature of the rock if no phase changes occur but cannot predict the observed nonuniformity of energy deposition. In all rocks shocked to higher pressure than was necessary to close the voids, high-pressure and/or high-temperature phases are present. Locally high pressures enduring for microseconds and high temperatures enduring for milliseconds controlled the phases of SiO_2 that formed in the rock. Collapsing pore walls became local hot spots into which initial deposition of energy was focused. Microcrystalline coesite in class 2 rocks occurs in symplektic regions on quartz grain boundaries that were regions of initial stress and energy concentration, or in sheared zones within the grains. The occurrence and morphology of the coesite-rich regions can be explained only if the transformation from quartz to coesite proceeds slowly in the shock wave. In class 3 rocks, microcrystalline coesite occurs in opaque regions that surround nearly isotropic cores of cryptocrystalline coesite. The cores are interpreted to be the products of the inversion of stishovite (or a glass with Si in sixfold coordination) that initially formed in the shock front in regions of grains shocked to pressures near 300 kb. Stishovite is preserved only in the opaque regions, which are believed to have been cooler than the cores. In class 4 rocks vesicular glass occurs in core regions surrounded by opaque regions containing coesite. The relation of the glass to the coesite and quartz suggests that the glass was formed by inversion of stishovite formed above 350 kb on release to lower pressure. Class 5 rocks are composed almost entirely of glass, with vesicles uniformly distributed in the glass. These vesicles were probably formed by exsolution of water that had been dissolved in melted SiO_2 during passage of the shock.

A study of the shocked Coconino sandstone from Meteor Crater, Arizona, was undertaken

to investigate the process of shock-wave propagation through a porous, granular medium and the effect of voids on the shock wave and the formation of high-pressure phases. The study of shock processes in porous media is important because nearly all known terrestrial and suspected planetary erosion processes act to fragment and disintegrate planetary surfaces, and, for this reason, a large proportion of impact
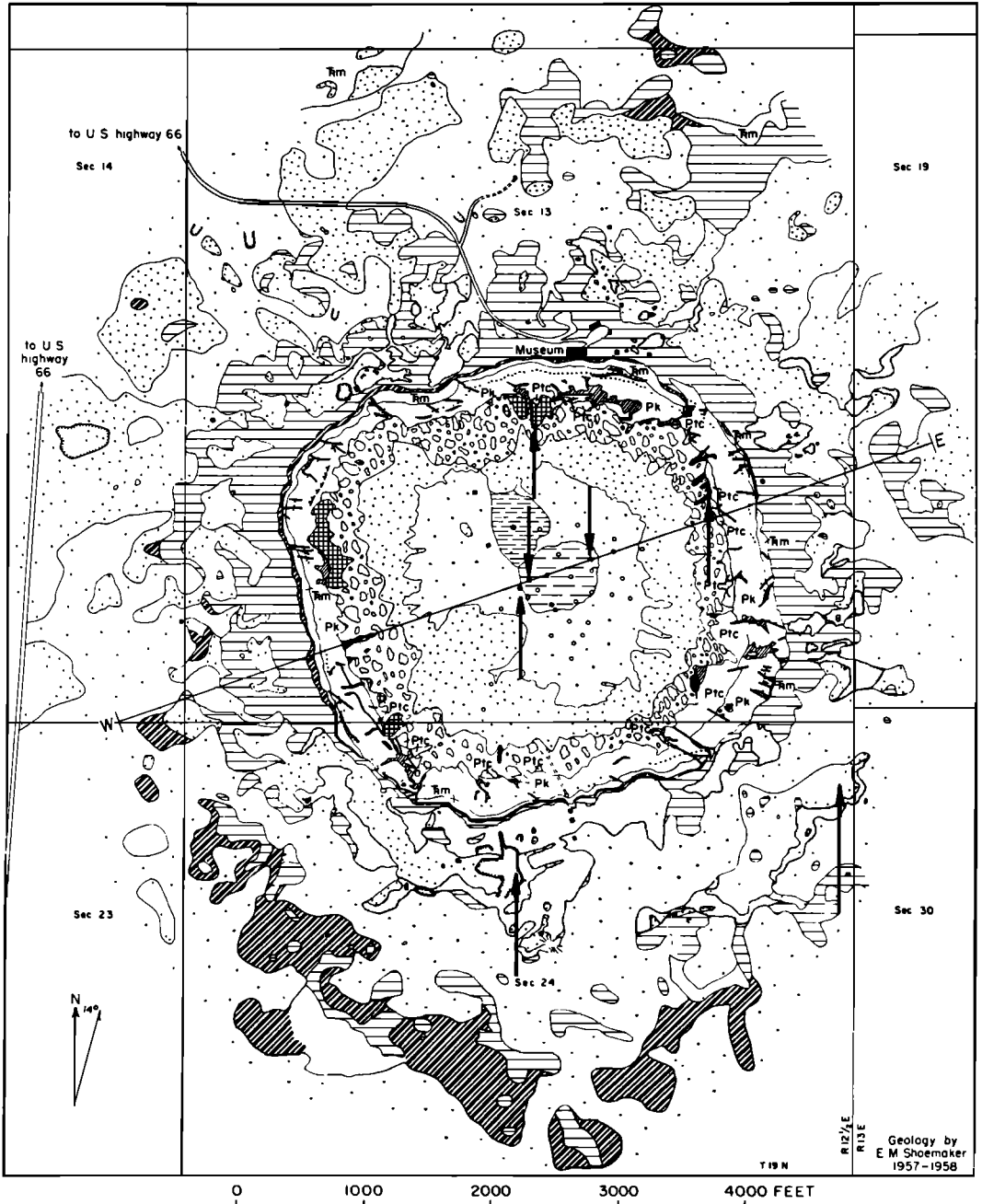
GEOLOGIC MAP OF METEOR CRATER, ARIZONA

Fig. 1. Geologic map of Meteor Crater, Arizona (courtesy of E. M. Shoemaker), showing structure of the crater, debris units containing shocked Coconino, and the location of sample-collecting areas (arrows).

EXPLANATION

Recent {

Alluvium   Playa beds

UNCONFORMITY

Pleistocene

Alluvium

Talus

Lake beds

UNCONFORMITY

QUATERNARY

Mixed debris from Coconino, Toroweap, Kaibab, and Moenkopi formations, includes lechatelierite and meteoritic material

Debris from Coconino sandstone and Toroweap formation

Debris from Kaibab limestone

Debris from Moenkopi formation

UNCONFORMITY

Trm

Moenkopi formation

TRIASSIC

UNCONFORMITY

Pk

Kaibab limestone, dotted line is sandstone bed

PERMIAN

Ptc

Toroweap formation and Coconino sandstone

Contact

Faults, nearly vertical or normal

Thrust fault, teeth are on side of upper plate

Authigenic breccia, fragments not mixed, occurs mostly along faults

Allogenic breccia, fragments mixed, includes lechatelierite and meteoritic material

Shaft

Adit

Pit

Dump

Drill hole

Explanation of Figure 1

events produce shock waves that traverse porous, granular materials. Terrestrial craters such as Meteor Crater (Arizona), Campo del Cielo (Argentina), Gosses Bluff (Northern Territory, Australia), Henbury (Northern Territory), and Wabar (Arabia) contain the products of shock metamorphism of granular materials. To interpret the record of impact on a planetary surface, it is necessary to be able to relate the observed shock-produced changes to the initial state of the surface material and to the pressure, temperature, and duration of the shocks to which it has been subjected.

The Coconino sandstone from Meteor Crater, Arizona, was selected for this study because naturally occurring shocked samples are readily available at the crater. These samples, which have been subjected to a range of shock pressure and temperature histories, represent a broad range of final states that result from a meteorite impact. The Coconino sandstone is composed almost entirely of quartz, the only mineral for which sufficient data exist to allow an interpretation of the complex behavior that results from shock loading.

METEOR CRATER AND THE COCONINO SANDSTONE

Meteor Crater (Figure 1) lies in the Canyon Diablo region of the southern part of the Colorado Plateau. The crater was formed in sedimentary rocks (the Coconino sandstone, Toroweap, Kaibab, and Moenkopi formations) ranging from Permian to Triassic age. The rim of Meteor Crater is blanketed by an overturned flap (with inverted stratigraphy) ejected from the crater; this, in turn, is overlain by Pleistocene and Recent alluvium (Figure 1; *Shoemaker* [1960, 1963]). The lower walls and floor of the crater are covered by Pleistocene and Recent deposits. Talus along the crater walls grades into alluvium on the floor of the crater, which, in turn, interfingers with a series of lake beds about 30 meters thick. These deposits overlie a layer of thoroughly mixed debris (the fallout) composed of fragments of Coconino sandstone, Toroweap, Kaibab, and Moenkopi formations, and meteoritic fragments. The mixed debris unit (attributed by Shoemaker to fallout of debris thrown to great height) is exposed in the crater walls and has been penetrated by several shafts in the bottom of the

crater. The mixed debris on the crater floor is underlain by a breccia composed of fragments of Coconino sandstone.

The Coconino sandstone underlies 8.3×10^4 km^2 of the Colorado Plateau province in northern Arizona. At Meteor Crater, outcrops of Coconino are best seen on the southeast wall, but small outcrops also occur on the north, east, and south walls. The nearest exposures outside the crater are 24 km to the south. The upper part of the Coconino as exposed at Meteor Crater is a pale buff, white, or pink cross-bedded sandstone. The coarseness of the cross bedding causes a massive appearance in outcrop. It is convenient to recognize two types of sandstone in hand specimen and thin section: (1) massive sandstone, in which laminations, if they exist, are several centimeters thick; and (2) laminated sandstone, containing parallel laminations that are 0.5 to 2 mm thick. The widest variations of mineralogy, porosity, and grain size are associated with these laminations.

The observed detrital constituents of the Coconino sandstone include [Kieffer, 1970] quartz, feldspars (<1%), rock fragments (<2%), and heavy minerals (<2%). The rock fragments are quartzites, siltstones and igneous or metamorphic crystalline fragments. Recrystallized quartz, chlorite (<2%), sericite and clay minerals (<5%), and hematite and

goethite occur as secondary minerals. McKee [1934] reported zircon, green tourmaline, blue tourmaline, leucoxene, monazite, rutile, magnetite, and anatase in total amount less than 0.2% in the Coconino in northern Arizona. Recrystallized quartz is the primary cement in the Coconino at Meteor Crater.

The detrital grains of the Coconino are well rounded (about 0.7–0.8 on the scale proposed by W. C. Krumbein in 1941 for estimating roundness); see Figure 2. Including the secondary overgrowths, the grains are generally slightly elliptical in shape and may have angular boundaries. The boundaries of the detrital grains against secondary overgrowths of quartz are revealed by layers of dust and vesicles (Figure 2). The grains have reentrants only in those places where quartz has been dissolved from the boundaries. In this study, the shape of the grains was characterized by the ratio of two perpendicular diameters, one of which was the longest grain dimension. Measurements of this ratio, $d_{max}/d_{\perp}$, obtained in traverses of a typical massive specimen, yield a mean value of 1.5 with a standard deviation of 0.5 A somewhat wider variation of grain shapes is observed in the laminated rocks.

In a typical specimen of massive sandstone, the longest dimension of the grains in thin section was found to range from 0.09 mm to 3.90 mm, with a mean value of 0.19 mm. The size-frequency distribution is unimodal with the mode between 0.250 and 0.177 mm (2.0 and 2.5 ϕ units). Laminated sandstones typically show a bimodal size distribution with modes at longest grain diameters of about 0.1 mm and 0.2 mm.

In massive specimens, no orientation of the overgrown grains was observed. In bedded specimens, slight alignment of the long axes of detrital grains parallel to the bedding is preserved in the overgrown grains.

The ratio of pore space to grain space in thin sections of three typical massive rocks taken from the rim is 0.18, 0.16, and 0.09; the average porosity of laminated rocks, determined in this way, is considerably less and is generally less than 10%. Variation in porosity on both a large scale and a small scale (locally within a hand specimen or thin section) has a significant effect on the nature of the shock wave passing through the material [see Kieffer,
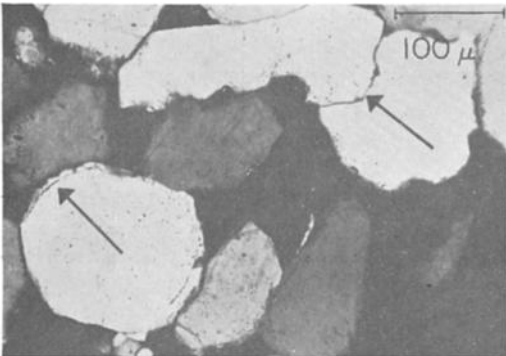

Fig. 2. Photomicrograph of quartz grains in unshocked Coconino. The boundaries between detrital grains and secondary quartz are marked by lines of inclusions, as shown by lower arrow. The boundary between the two white grains at the upper arrow is typical of the irregular, microstylolitic boundary formed by solution of the original detrital quartz (crossed Nicols).

1970]. The porosity varies over distances on the order of millimeters. To measure the distribution of distances of pore closure under shock compression, traverses were made across a typical thin section of massive sandstone, and the diameter of each pore encountered was measured in the direction of the traverse. The pore closure distances, measured in this way, range from less than 0.005 mm to nearly 0.4 mm. The mean closure distance is 0.04 mm (ϕ = 4.44), with a standard deviation of 1.36 ϕ units. The mean distance of separation of the pores is equal to the mean diameter of the quartz grains, 0.19 mm. Separations up to one millimeter are common; occasionally larger separations are observed.

In detail, the pore shapes are extremely complex and irregular; in some places, small channels connect the major pores. The pores are generally elongate, but the smaller pores may be equant. The shape of the pores is controlled by (1) the packing of the grains and (2) irregularities on the surfaces of the grains themselves. The latter effect is minor, except for sets of intersecting crystal faces on the secondary quartz, which form sharp corners on the pore wall. The three most frequent shapes of grain surfaces observed on a pore wall are (1) rounded (portions of approximately spherical or elliptical grains), (2) planar (recrystallized quartz faces), and (3) angular (intersecting crystal faces).

PREVIOUS STUDIES ON SHOCKED COCONINO SANDSTONE AND ON SHOCKED QUARTZ

Shock metamorphosed Coconino sandstone was first recognized at Meteor Crater by *Barringer* [1905], *Tilghman* [1905], and *Fairchild* [1907]. These early investigators recognized three types of shocked sandstone. One type consists of crushed and pulverized sandstone; the most extreme example of crushing is a fine quartz powder, 'white as snow,' consisting of minute fragments of sharp, angular quartz.

A second type, called 'variety A' by *Barringer* [1905, 1909], has a higher density than the original sandstone and a slaty structure at varying angles to the original rock lamination. *Merrill* [1907, 1908] in a microscopic study of these rocks recognized an extinction pattern in the quartz grains, which he suggested resulted from pressure on the grains while in a plastic

condition. *Merrill* [1908, p. 475] also observed 'small, colorless, interstitial areas showing by ordinary light a fibrous structure, but which are, for the most part, completely isotropic between crossed Nicols, and which the chemical analysis suggests may be opal.' These interstitial areas are shown in this work to contain high-pressure phases of SiO_2. Merrill recognized a 'marked rhomohedral cleavage' of quartz in these rocks; later studies by *Bunch and Cohen* [1964] suggested that the texture of these cleavages was sufficiently different from the texture of quartz deformed by other geologic processes to serve as an indicator of an impact event.

'Variety B' of the shock metamorphosed sandstone, as defined by the early explorers at Meteor Crater, has a very cellular, pumiceous structure. The density is so low that it will float on water. Under the microscope it was recognized to be composed mostly of amorphous silica, lechatelierite, with scattered particles of crystalline quartz. *Fairchild* [1907] suggested that there was sufficient water, perhaps in the joints of the strata, to effect aqueoigneous fusion. *Rogers* [1928] observed numerous minute bubbles in thin sections of the variety B glass and suggested that moisture originally present was converted to steam and was in part responsible for the vesicles.

Rogers [1928] recognized in the variety B rocks silica glass, which retained the structure of the sandstone from which it was formed and which he called 'paramorphs of lechatelierite after quartz.' *Chao* [1967] and *von Engelhardt et al.* [1967] have recognized glass with the same property and refer to it as thetamorphic or diaplectic glass.

Coesite [*Chao et al.*, 1960] and stishovite [*Chao et al.*, 1962] were first discovered as naturally occurring minerals at Meteor Crater in the variety A rocks and as a minor constituent in the variety B rocks. The stability fields of these high-pressure polymorphs are shown in Figure 3.

Since the early work of Rogers, Merrill and Barringer, investigators have discovered many properties of naturally or artificially shocked quartz which appear to be characteristic of shock loading. (For detailed reviews of shock features in quartz see *French and Short* [1968].) The following definitions are used to
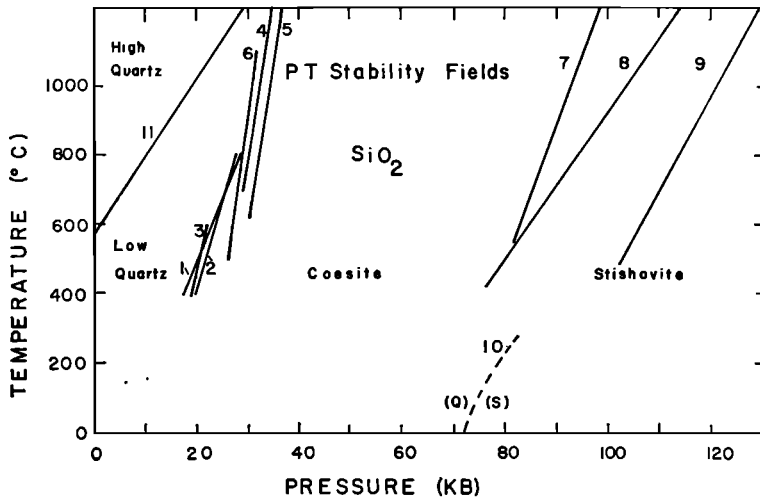
Fig. 3. Pressure-temperature stability fields of SiO₂. References from which the numbered curves were obtained are given in Table 1.

describe shock effects found in quartz in the shocked Coconino:

1. *Fractures:* irregular breaks in a grain, across which fragments are resolvably displaced; sometimes follow one or more cleavage planes.

2. *Cleavages and faults* (not differentiated, after *Hörz* [1968]; *Carter* [1968]): planar features that are 2 to 10 μ wide, spaced 20 μ or more apart from each other; parallel to planes of low crystal indices.

3. *'Planar features' and basal deformation lamellae* (not differentiated; referred to as 'planar features' after *Hörz* [1968]): very thin planar structures (1 to 2 μ or less in width), closely spaced (2 to 5 μ apart), occurring in sets of more than 5 individuals or in multiple sets.

4. *Thetamorphic (or diaplectic) glass* (after *Rogers* [1928]; *Chao* [1967]; *von Engelhardt et al.* [1967]): optically isotropic SiO₂ with an index near that of normal glass, occurring in the morphology of the original or part of the original quartz grain. Flow structures and vesicles are absent.

5. *Lechatelierite or fused silica:* optically isotropic SiO₂ with an index 1.46, showing flow structures or vesicles.

6. *Coesite:* monoclinic phase of SiO₂ stable between approximately 30 kb and 75 kb at 300°K (Figure 3 and Table 1), density 2.92

g/cm³ at STP and mean index 1.594 [*Skinner and Fahey*, 1963].

7. *Stishovite:* tetragonal phase of SiO₂, stable above 70 kb at 300°K (Figure 3), with density of approximately 4.3 g/cm³ and mean index 1.806 [*Skinner and Fahey*, 1963].

TABLE 1. Sources of Data for SiO₂ Stability Fields

Number[*]	Transition	Reference
1	Quartz to coesite	*Griggs and Kennedy* [1956]
2	Quartz to coesite	*MacDonald* [1956]
3	Quartz to coesite	*Dachille and Roy* [1959]
4	Quartz to coesite	*Boyd and England* [1960] *Boyd et al.* [1966]
5	Quartz to coesite	*Takahashi* [1963]
6	Quartz to coesite	*Kitahara and Kennedy* [1964]
7	Coesite to stishovite	*Akimoto and Syono* [1969]
8	Coesite to stishovite[†]	*Stishov* [1963]
9	Coesite to stishovite	*Ostrovsky* [1965, 1967]
10	Quartz to stishovite[‡]	*Holm et al.* [1967]
11	High to low quartz	*Cohen and Klement* [1967]

  * Numbers correspond to numbers on curves in Figure 3.
  † Estimated.
  ‡ Calculated.

OCCURRENCE OF SHOCKED COCONINO

The distribution of ejecta including shocked Coconino sandstone at Meteor Crater was first described and mapped by *Shoemaker* [1960]. Fragments of shocked Coconino sandstone are found in the Coconino sandstone debris unit, the breccia under the crater floor, the mixed debris unit (fallout), and in the alluvium and lake beds; these units are shown in Figure 1. Shocked material from the breccia, the mixed debris, and the lake beds underlying the crater floor is presently accessible in the dumps adjacent to the shafts on the floor of the crater (Figure 1, center of crater).

Each of the units mentioned above has particular types of shocked material in it. The breccia underlying the crater bottom is composed of fractured and crushed Coconino sandstone and includes dispersed fragments containing coesite. The mixed debris unit is an especially rich source of shocked sandstone containing coesite and stishovite. The lowermost Pleistocene lake beds contain abundant fragments of pumiceous shock-melted sandstone. Abundant fragments of shocked sandstone containing coesite and stishovite and pumiceous shock-melted material are found in the alluvium surrounding the crater. The alluvium was derived from mixed debris and also from the stratified debris units of the crater rim. Silica pits on the south side of the crater are a source of very weakly shocked sandstone from the Coconino sandstone debris unit.

Samples for these studies were collected from three shaft dumps in the center of the crater, two exposures of mixed debris on the crater walls, the silica pits, and an alluvial terrace on the south side of the crater. These locations are shown by arrows in Figure 1.

CLASSIFICATION OF THE SHOCKED ROCKS

From several hundred pounds of shocked Coconino, 48 rocks were selected for thin section examination. From these, 16 rocks representative of varying degrees of shock metamorphism were selected for measurement of silica polymorph abundances by X-ray diffraction.

Some of the rocks collected from Pleistocene alluvium contain abundant calcite in fractures and vesicles. This calcite was deposited in the rocks by soil-forming processes during late Pleistocene time (E. M. Shoemaker, personal communication). The calcite is not relevant to the shock history of the rocks and was extracted before measurements of the SiO_2 polymorph abundances were made.

The abundances of quartz, coesite, stishovite, and glass were determined by techniques of quantitative X-ray diffraction described in *Keiffer* [1970]. Abundances were determined with a relative error of less than 10%. The results of the X-ray diffraction measurements, shown in Figure 4, provide a convenient basis for classifying the specimens of shocked Coconino. The suite of shocked rocks is divided into five classes, arranged in order of decreasing quartz content. Boundaries between the classes are chosen approximately halfway between adjacent data points in Figure 4. The five classes are denoted by the numerals 1, 2, 3, 4, and 5, and subclasses are denoted by small Arabic letters a and b. The classes are:

Class 1. Weakly shocked rocks containing no high-pressure phases and 95% or more quartz (a) with petrographically observable remnant porosity; (b) without petrographically observable remnant porosity.

Class 2. Moderately shocked rocks containing 80 to 95% quartz. These rocks typically have 2 to 5% coesite, 3 to 10% glass, and no detectable amount of stishovite.

Class 3. Moderately shocked rocks containing 45 to 80% quartz. These rocks typically have 18 to 32% coesite, trace amounts of stishovite, and 0 to 20% glass.

Class 4. Strongly shocked rocks containing 15 to 45% quartz. These rocks typically have 10 to 30% coesite, 20 to 75% glass, and no detectable stishovite.

Class 5. Very strongly shocked rocks that contain 0 to 15% quartz. These rocks may have 0 to 5% coesite, 80 to 100% glass, and no detectable stishovite.

Rock fabric and texture are strongly correlated with this mineralogical classification and 45 of the 48 rocks examined in thin section could be placed in one of the five classes on the basis of their microscopic or hand-specimen appearance alone. Three remaining rocks were either class 3 or class 4 and appeared anomalous in their petrographic properties; these three rocks plus rock 16 (Figure 4) appear to be class 3 rocks with atypically high glass contents. The three rocks have not yet been studied in detail.
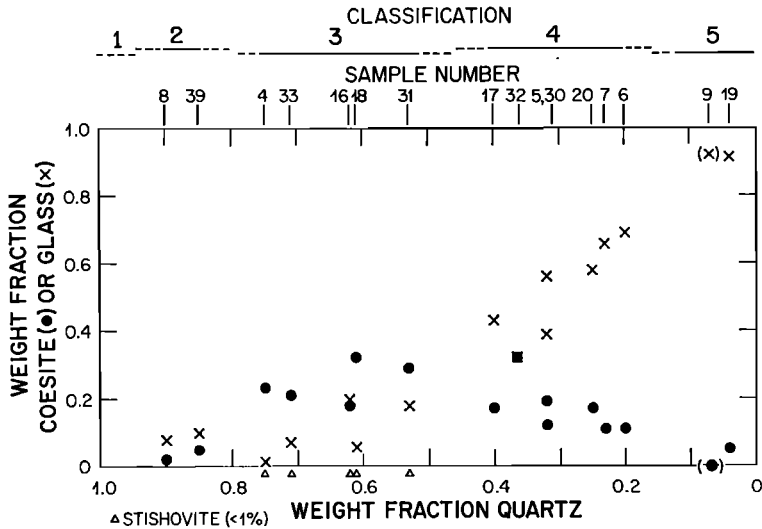
Fig. 4. Abundance of coesite (●) and glass (×) in shocked Coconino sandstone as a function of quartz content. Rocks in which stishovite was detected (greater than 0.25% and less than 1% by weight) are indicated by a triangle. Limiting quartz contents of 5 classes of rocks are shown on top line. Sample numbers of rocks are also shown at top of graph.

Class 1a rocks. Samples of class 1a rocks were collected from the dumps at the shafts in the center of the crater and from the silica pit on the south side of the crater. In general, specimens of weakly shocked rocks with remnant porosity do not differ in macroscopic appearance from unshocked Coconino sandstone. They are granular (0.1 to 0.2 mm average grain size), weakly to moderately cemented, and may be either massive or laminated.

In thin section, these rocks characteristically show less porosity than massive unshocked Coconino, generally having less than 5% porosity. The reduction of porosity in class 1a rocks apparently occurred by slight translation and rotation of individual grains or small groups of grains. Irregular fractures may exist in up to 5% of the grains. Wavy extinction under crossed Nicols occurs in less than 5% of the grains. Planar features do not occur in class 1 rocks.

Class 1b rocks. Class 1b rocks were collected from the mixed debris or breccia in the shaft dumps in the center of the crater. When the dumps are moist, some of these rocks are nearly indistinguishable from the fines and can be easily overlooked. When allowed to dry, they become coherent, though fragile, fine-grained and friable. Other class 1b rocks, although

powdery in texture, retain their coherence when wet. These rocks are snow white in hand specimen and are generally less than 5 cm in longest dimension. Undistorted laminations can be seen on some hand specimens. Individual grains are easily resolved with a hand lens.

Fracturing of grains occurs irregularly throughout 1b rocks. Disoriented shards frequently form nests or pockets between large quartz grains. Over 40% of the fractured quartz grains retain their continuity, even though most of the grains have 5 to 10 fractures within the grain outline. Remnant lines of vesicles associated with the boundary between detrital grains and quartz overgrowths are commonly visible on grains that have been undamaged, on grains that have been fractured, and on rotated chips.

Fractures in the grains that have retained their continuity can generally be related to surfaces of contact with other grains. Extensive networks of radial fractures emanate from the contact surfaces of up to 20% of the grains (Figure 5). These fracture systems are here termed *concussion fractures* because of their resemblance to fracture systems produced by hypervelocity impact in solid rock, and the line joining the centers of pairs of grains that show concussion fractures is here called the *apparent*

concussion axis of these grains. A set of three mutually perpendicular thin sections was made from a moderately laminated class 1*b* rock that showed concussion fractures. The orientation of the three thin sections is shown schematically on the cube in Figure 6. The directions of the apparent concussion axes were measured in each of the thin sections. The results are shown on the foldout of the cube OABCGDE in Figure 6 and on the polar plots adjacent to the foldout; 72 apparent concussion axes were measured in thin section 1, 33 in section 2, and 27 in section 3. As shown by the polar plots, the axes of sections 1 and 2 are aligned to within ±15° and ±20°, respectively, of the median value. A concentration of about 10 axes/mm² appears desirable to obtain a representative median value of the axial direction in thin section; the assignment of a median direction for sections 3 and 2 may not be statistically significant.

The radial concussion patterns are believed to be tensile fractures formed by the impact of neighboring grains as the shock front initially traversed the material and closed pore spaces. A qualitative idea of stress concentrations in sand grains impacting at low velocities can be obtained from consideration of the collision of two perfectly elastic spheres of identical size and properties [*Hertz*, 1896; *Timoshenko and Goodier*, 1970; *Kieffer*, 1970]. At the time of maximum deformation of the two spheres, the maximum pressure is obtained at the center of the surface of contact (the surface that is common to the two bodies when in closest contact). The compressive stress decreases along the concussion axis toward the centers of the grains. The maximum tensile stress occurs at the circular boundary of the surface of contact. It is radial to the center of the surface of contact in the plane of the surface of contact. For a brittle material, such as quartz, tensile fractures would tend to form normal to the maximum tensile stresses and would therefore form concentric to the boundary of the contact surface. Divergence of the tensile stress field with distance away from the contact surface would probably cause the tensile fractures to have the appearance of cones, truncated at the contact surface and diverging into the grains. A cross section of this pattern would give fractures that diverge radially from

the contact surface into the grain; this is the idealized pattern of fractures seen in the grains with concussion fractures in class 1*b* rocks. The details of the observed patterns may depend critically on local geometry at the point of initial impact.

These fractures must have been formed before the mean pressure in the sandstone became large, that is, in the impact of sand grains due to the first shock. Thus the median value of the axial direction is believed to be nearly the direction of passage of the shock through the material. The concussion axes do not provide a vector direction, hence the shock may have propagated in either direction along the median.

Class 2 rocks. The class 2 rocks examined came from the mixed debris unit. In hand specimen they are white, generally are smaller than 5 cm in longest dimension. They are well-indurated and dense. Most class 2 rocks are traversed by small parallel partings whose separation does not exceed 0.1 mm. Individual grains are generally not resolvable with a hand lens.

In thin section, quartz grains are observed to be fractured throughout and altered on the boundaries. The grains, which are approximately the same size as the original grains, cover 80 to 95% of the area of the thin sections. There is no petrographically observable porosity in these rocks, and the quartz grains interlock with
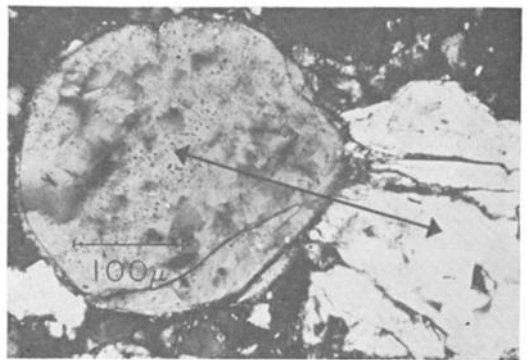

Fig. 5. Concussion fractures emanating from contact surface between two grains on class 1*b* rock. Small amounts of fine-grained material were forced into the radiating fractures. The apparent concussion axis is shown by arrows. Vesicles marking the boundary between the left detrital grain and secondary quartz have not been destroyed and are visible on the left and lower edge of the grain.
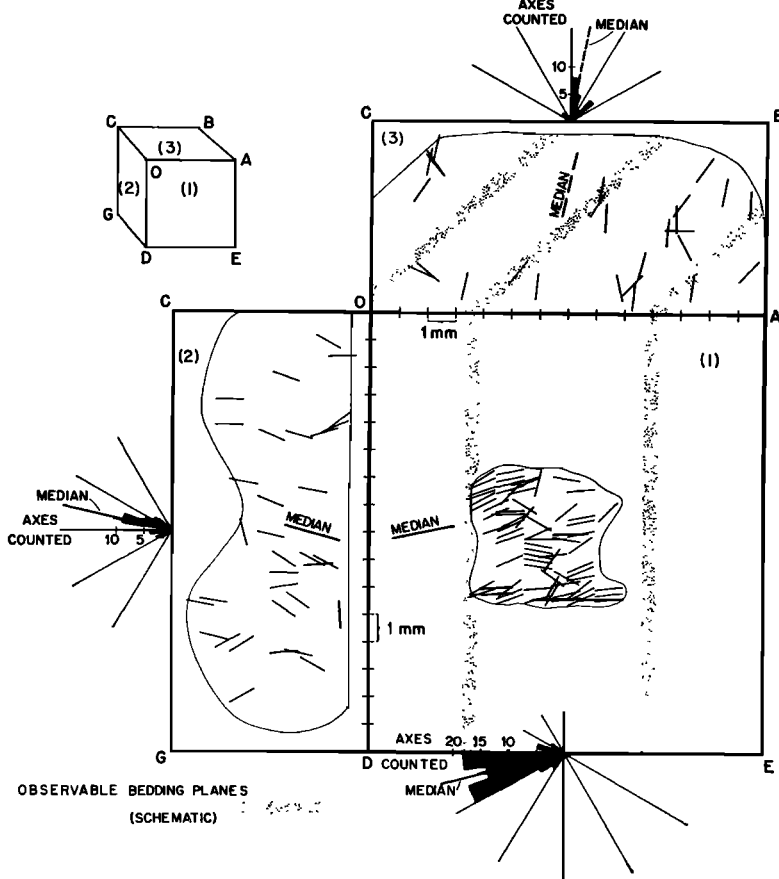
Fig. 6. Cube AODEGCB shows orientation of three orthogonal thin sections cut from class 1b rock to study concussion fractures. Foldout shows orientation of apparent concussion axes in the three thin sections; outlines and relative sizes of thin sections are shown to scale. Polar plots show distribution of axial directions and median direction.

one another like pieces of a jigsaw puzzle (Figure 7). Lining parts of the boundaries of the grains are areas that appear yellow to gold in transmitted light and scatter reflected light. These regions (5 to about 50 μ wide and up to 0.2 mm in length) are composed of submicron to micron-sized, high-index crystallites, isotropic areas, and quartz, which is generally visible in optical continuity through the regions (Figure 7). The minerals, intermixed within microns, appear in a vermicular habit, for which reason they are herein called *symplektic regions*.

In contrast to the class 1b rocks, in which the grain size is reduced from that of the unshocked Coconino by fracturing, the average grain size of the quartz in class 2 rocks is similar to the grain size in unshocked rocks (a

typical average longest-grain dimension is 0.18 mm, as compared to 0.19 mm in a typical, massive unshocked rock).

Quartz grain shapes in class 2 rocks are different from grain shapes in any observed unshocked rock (Figure 7). Many of the grains are irregular, containing gentle re-entrants. The grain-shape parameter is 1.8, indicating that the grains are somewhat more elongated than the original grains, for which the grain-shape parameter was 1.5. The direction of elongation of quartz grains in class 2 rocks is aligned to within ±20° of the median value (Figure 8). This alignment of long axes is also present in class 3 rocks containing more than 60% quartz. Consideration of the net one-dimensional strain imparted to these rocks during shock compres-

sion suggests immediately that the direction of grain elongation is tangential to the direction of the shock front. Thus, criteria is available in class 1*b*, class 2, and some class 3 rocks for determining the direction of shock passage. In rock with less than 60% quartz, phase changes have extensively modified the original grains, and similar patterns of alignment do not exist.

The change in shape of the quartz grains without fracturing, combined with extensive strain indicated by wavery extinction in the grains, suggests that extensive plastic deformation of the grains occurred as they were compressed and squeezed into pore spaces. Plastic deformation at the grain boundaries appears to have eliminated the small vesicles marking the boundary between detrital sand grains and crystalline overgrowths.

Over 90% of the quartz grains are permeated with sets of cleavages. Planar features were observed on less than 5% of the grains. The orientation of cleavages and planar features was not studied.

The symplektic regions were determined by methods of Debye-Scherrer X-ray photography, to contain coesite. The coesite is generally visible as high-index crystallites less than 2 μ in diameter, here called *microcrystalline coesite*. It was measured in two class 2 rocks to be 2 and 5% by weight.

These rocks contain 8 to 10% glass. Low-index, isotropic regions of thetamorphic glass are observed (Figure 7) and may comprise up to a few per cent of the rock, but in general the glass must occur in unresolved domains within the symplektic regions, since this abundance of glass cannot be petrographically identified.

The symplektic regions are generally elongated tangential to quartz grain boundaries for distances up to 0.2 mm but are only 5 to 50 μ in width perpendicular to the boundary. The distribution of distances between symplektic regions is similar to the distribution of pores in the unshocked rock (Figure 9). The resemblance between the distribution of pores and the distribution of symplektic regions, when considered with the occurrence of the symplektic regions only at grain boundaries, and the elongation of the regions tangential to the grain boundaries suggest that the symplektic regions line the walls of collapsed pores.

Class 3 rocks. Specimens of class 3 rocks were collected on the alluvial terrace on the south side of the crater and from the mixed debris unit. All class 3 rocks are well indurated and dense. They all display a platy structure, but the structure is better developed in some rocks than in others. Individual grains are not resolvable with a hand lens.

In thin section, the following regions of SiO_2 with different properties can be identified: (1) quartz grains; (2) high-pressure phae regions, which include (a) symplektic regions on quartz boundaries, (b) opaque regions grading into the symplektic regions over a distance not exceeding 10 μ, and (c) high-index cores within some opaque regions. The typical occurrence of these regions is shown in Figure 10.

Quartz comprises 45 to 80% of the area of the thin sections and occurs as remnant grains. Quartz grains are generally between 0.1 and 0.3 mm in diameter in these rocks. Less than 5% of the thin-section area is covered by regions of quartz chips less than 0.05 mm. On the order of 10 to 20% of the quartz grains cannot be distinguished from their neighbors under crossed Nicols because wavy extinction prevents definition of the boundaries. The grains were apparently plastically deformed around each other to fill the void space as the rock was compressed.

Planar features were observed in about 5%

Fig. 7. Photomicrograph (crossed Nicols) showing jigsaw texture due to plastic deformation of quartz grains on a class 2 rock. Center grains have re-entrants on boundaries due to deformation. Arrows point to symplektic region (1) and to isotropic region (2) on grain boundary. The isotropic region probably contains an unresolvable mixture of coesite and diaplectic glass. Cleavages are visible on the grains. Emulsion is streaked in center of photograph.
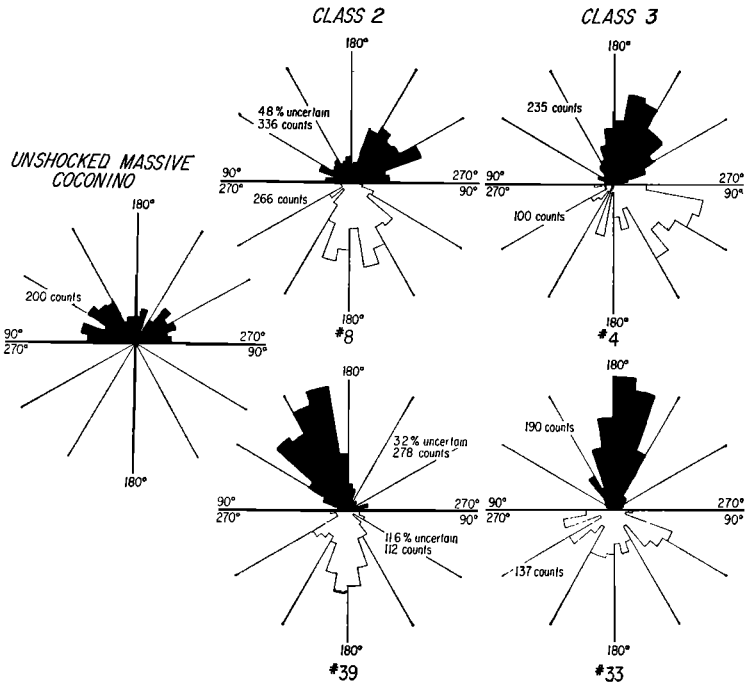
Fig. 8. Shaded polar plots show the orientation of long grain axes in a typical massive un-shocked rock, two class 2 and two class 3 rocks, and demonstrate that a preferred orientation of long axes exists in the shocked rocks. Unshaded plots show direction of elongation of symplektic regions (class 2 rocks) or opaque regions (class 3 rocks) and demonstrate that, if alignment of the regions containing high-pressure phases exists, it is not in the same direction as the alignment of long grain axes.

of the grains. All quartz grains are permeated with cleavages. The orientation of cleavages in class 3 rocks is, according to *Bunch and Cohen* [1964], in order of decreasing abundance, {1011} or {0111}, {0001}, {1010} or {1120}, and {1122}.

Nearly every quartz grain in class 3 rocks is surrounded by a 10 to 40-μ-wide symplektic region containing high-index coesite crystallites up to 2 μ in diameter. The large symplektic regions penetrate deeply into quartz grains, sometimes following cleavage directions. Symplektic regions are also found as linear features separating regions of a quartz grain that have differing extinction properties. These regions have been rotated to differing optical orientations; the coesite apparently formed along the zone of strongest shear. A few per cent of the symplektic regions are associated with regions of isotropy that may be thetamorphic glass.
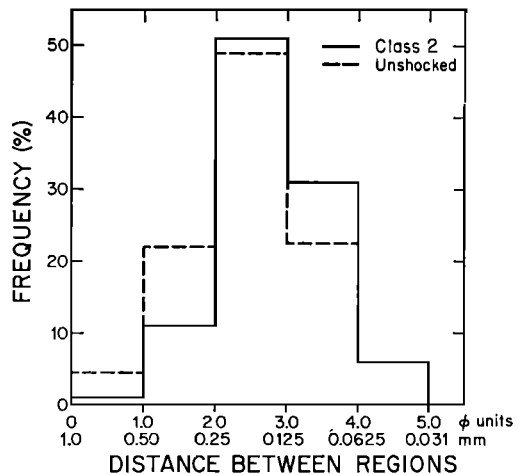

Fig. 9. Frequency distribution of distance between pores in typical massive unshocked rock (dashed line) and between symplektic region in class 2 rock (solid line).
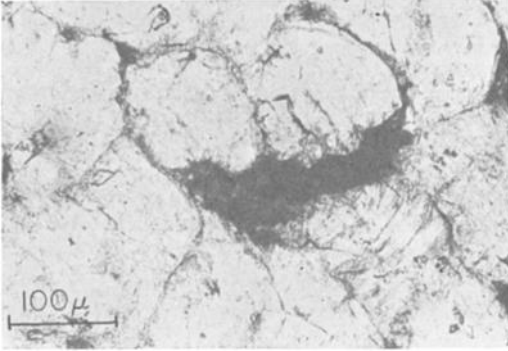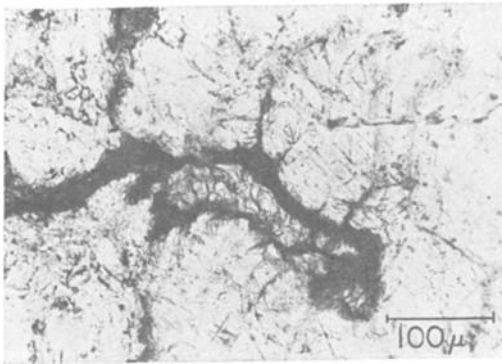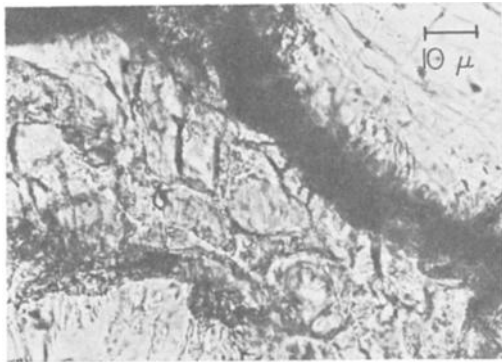
Fig. 10a.

Fig. 10b.

Fig. 10c.

Fig. 10. Photomicrographs showing the typical occurrence of high-pressure phase regions in class 3 rocks (plane polarized light). (a) Elongated, opaque region (black) surrounded by (grey) symplektic material interfingering with (white) quartz grains. (b) Opaque border (black) surrounding cryptocrystalline coesite core (clear). (c) The same core and opaque border showing cellular structure within core.

The symplektic regions grade into opaque regions that assume two characteristic shapes. Smaller regions are generally elongated and entirely opaque (Figure 10a). Larger regions frequently form an elliptical border (adjacent to the symplektic regions of the quartz grains) surrounding a core of high-index and extremely faint birefringence (Figures 10b, and 10c). The opaque regions, in thin section or as crushed grains in immersion oil, scatter reflected light diffusely and can be easily identified by this property. Debye-Scherrer X-ray photography showed that coesite always occurs in these regions and stishovite occurs in some of the opaque regions. Stishovite was only found in the opaque regions. These opaque regions were erroneously reported by *Bunch and Cohen* [1964] to contain iron oxides; microprobe scans of these regions showed no iron was present. The cause of the opacity of these regions is discussed in a later section of this paper.

Cores located within the opaque regions are usually 60 to 100 μ in longest dimension, but occasionally are as large as 200 μ. Small crystallites, presumably of microcrystalline coesite, are found in the outer regions of the core in the same vermicular habit that occurs on the quartz boundaries. This relationship indicates that the cores were formed before the microcrystalline coesite. The cores are seldom structureless; rather, they are pervaded by a network of fractures that subdivide them into smaller 'cells' that are generally less than 20 μ in diameter, (Fig. 10c). The cells are usually round to oblate in shape.

The index of four cores extracted from crushed grains in immersion oil is 1.584 ± 0.004; Debye-Scherrer X-ray photography of the cores (20–40 μ in diameter) yielded weak coesite lines. The cores are nearly isotropic, generally showing variable and faint birefringence. The low birefringence and nonuniform distribution of the birefringence suggest that these cores are cryptocrystalline coesite. The grain size is substantially less than 1 μ; this habit of coesite is distinctly different from the microcrystalline coesite seen in the symplektic regions. Since the measured index of refraction is slightly lower than the reported indices of coesite ($\alpha = 1.599$, $\gamma = 1.604$ [*Coes*, 1953]), it is possible that small amounts of glass are present in the region.

Fig. 11a. Sketch of the typical occurrence of the four different SiO_2 regions in a class 4 rock: quartz grains (white), opaque rims (black) on many of the quartz grains, and a vesicular glass core (striped) surrounded by the opaque rim. A few symplektic regions (dotted pattern) are shown schematically on the quartz grains.

Class 4 rocks. Class 4 rocks were collected on the south terrace and from the shaft dumps, where they were probably derived from the mixed debris unit. They are usually distinguishable by their elongated, aligned fractures or vesicles. Remnant laminations are visible on some hand specimens. The laminations may be warped through an angle of 5° to 10° and may appear to be inflated; that is, they appear to have expanded in a direction perpendicular to the bedding.

In thin section, five regions with differing optical properties in these rocks are observed: (1) remnant quartz grains, (2) symplektic regions, (3) opaque regions, (4) vesicular glass cores, and (5) calcite.

The typical relationship between the first four of these regions is shown in the sketch in Figure 11a. Remnant quartz grains and fragments of grains are observed to cover 20 to 40% of the area of the thin sections. The grains appear to be floating in a sea of opaque material and vesicular glass; only 20 to 30% of the grains are in contact with other quartz grains. Nearly every grain is rimmed with a thin symplektic region and a border of opaque material. The opaque material frequently forms a continuous border up to 50 μ in width around 10 to 20 quartz grains and resembles a black ribbon tying together the grains. Adjacent to this black ribbon and frequently interior to it are found large areas of vesicular glass, forming cores within the opaque rims (Figure 11b).

Calcite pervades the rock in fractures and vesicles; it was deposited in the rocks as they weathered on the alluvial slopes. It is fine grained, highly birefringent, and is often finely laminated in contorted shapes in its occurrence within fractures.

As occurred in class 2 and class 3 rocks, small high-index crystallites are visible in the symplektic regions; they are assumed to be coesite. Debye-Scherrer X-ray photography of the opaque regions showed them to be rich in coesite. Cryptocrystalline coesite and stishovite were not found in the class 4 rocks.

Melted silica glass in the shocked Coconino sandstone occurs only in class 4 and class 5 rocks. The melted glass occurs in vesicular isotropic regions within the opaque rims (Figure 11b). These regions may be up to 3 mm in longest dimension. The glass is filled with vesicles that are observed from 2 μ to 0.1 mm. Most vesicles are less than 10 μ in diameter and occur so profusely as to cause an opacity in parts of the core similar to the coesite-rich opaque areas. Some vesicles are flattened and appear to have been sheared.

The presence of vesicles in the glass regions indicates that a gas was present as pressure on the rock was released. Of the three possible vapors (SiO_2, air, water), it is most likely that water vapor was associated with the vesicles [*Kieffer*, 1970]. The presence of sheared vesicles and fibrous bridges across vesicles indicates that this glass was fluid at relatively low pressure. This implies that, if the rock were dry, temperatures of approximately 1700°C existed in these regions on release of the rock
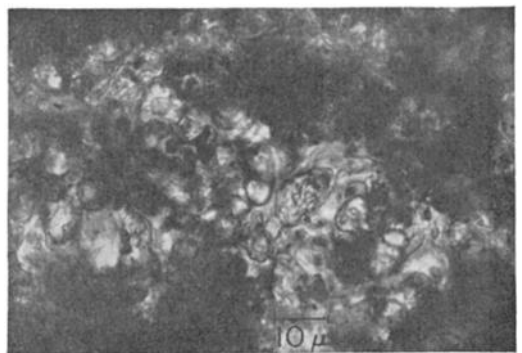

Fig. 11b. Photomicrograph of vesicles in glass in core region surrounded by opaque (black) coesite-rich region.

to low pressures. If the rock were wet, the temperature may have been as low as 1100°C [*Kennedy et al.,* 1962].

The vesicles are thoroughly interspersed in the SiO_2 glass, an observation that poses the problem of finding the mechanism by which water that was originally interstitial could get into the interior of melted grains. Kennedy et al. demonstrated that a critical end point for the univariant equilibrium melting curve of the SiO_2-H_2O system exists at 9.7 kb and 1080°C. Thus, at pressures greater than 10 kb and temperatures greater than 1100°C, complete intermixing of the SiO_2 and H_2O phases occurs. If water were incorporated into the SiO_2 at pressures above 10 kb, some water would exsolve and form vesicles on release to zero pressure. These observations on the existence of vesicles and on the proximity of fused SiO_2 to quartz suggest that water in the pores of the rock initially may have played an important role in allowing parts of the rock to melt at relatively low temperatures because they were wet, although other (dry) parts of the rock were not exposed to melting temperatures. The opacity of some of the glass due to minute vesicles suggests that vesicles cause the opacity of the opaque regions bearing microcrystalline coesite. Transmission electron microscope studies of these regions are now being conducted to investigate this hypothesis.

Rocks of classes 2, 3, 4, and 5 are well indurated and cohesive. Yet the secondary quartz that cements the unshocked rocks is broken or transformed in the process of pore closure. Some cohesion is provided by the high-pressure and high-temperature phases formed along the grain boundaries. Phase transformations and chemical reactions (such as dehydration) at grain boundaries may be a major mechanism of hock lithification of soils or porous rocks.

Class 5 rocks. Class 5 rocks consist primarily of glass and are, in hand specimen, low density, vesicular, and nearly pumiceous in texture. Thin sections of these rocks show a flowed, stretched glass (lechatelierite) in which vesicles of all sizes exist (Figure 12). Remnant fragments of quartz grains are embedded in a matrix of vesicular SiO_2. The glass is frequently opaque owing to the presence of numerous vesicles smaller than 2 μ.

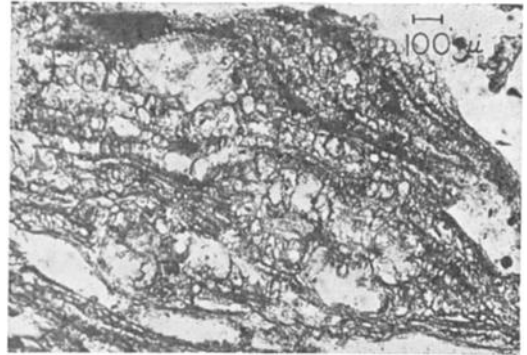Coesite was measured to comprise 5% of

Fig. 12. Photomicrograph (plane polarized light) of class 5 rock showing schlieren and fibrous bridges in glass (dark areas) and vesicles (light areas). In some regions vesicles are so dense as to cause opacity of rock (black regions).

one class 5 rock, it but could not be identified in thin section. By analogy with the occurrence of coesite in class 3 and class 4 rocks, it is expected that the coesite is located in close proximity to the quartz grains, rather than interspersed as crystallites within the glass. *Chao* [1968] reported that coesite is not found in rocks in the Ries basin, in which lechatelierite is observed. Coesite in close proximity to the lechatelierite in class 4 and class 5 rocks from Meteor Crater is apparently associated with the presence of pores in the unshocked rocks.

SHOCK-WAVE CONDITIONS AT METEOR CRATER

The shock wave generated by the impact event at Meteor Crater consisted of a relatively sharp rise to peak pressure, *the shock front,* and a slower decay to ambient pressure, the *rarefaction* [*Shoemaker,* 1963; *Bjork,* 1961]. The shock structure is shown schematically in Figure 13. The work done in increasing the internal energy of the rock mass by compression of the material is accomplished in the shock front. The release of shocked material to zero pressure occurs when the tail of release waves from the ground surface and the edges of the meteorite reach the shocked material. Pressures high enough to transform SiO_2 into high-pressure phases are maintained until the shock decays below approximately 30 kb in the rarefaction wave.

The time available for the formation of high-pressure phases may be estimated by considering separately the rise time to peak pressure
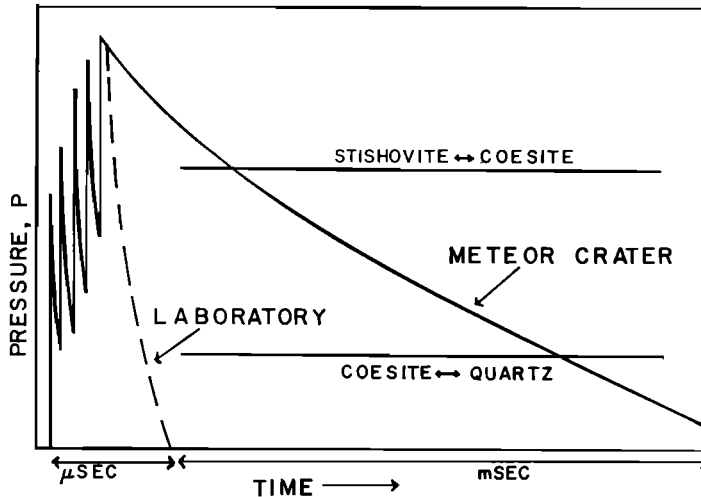
Fig. 13. Schematic diagram of shock structure at a point several hundred feet from the center of impact and of a laboratory shock event. Pressures at which phase boundaries are reached are indicated by horizontal lines; these are a function of pressure, temperature and reaction rate.

and the decay time to pressures of approximately 30 kb. The rise time is shown in the next section to be of the order of several microseconds. The decay time may be estimated by using the one-dimensional model of penetration mechanics developed by *Shoemaker* [1963] assuming a meteorite diameter of 30 meters (E. M. Shoemaker, personal communication) and a sound speed in SiO_2 at 30 kb pressure of 7.5 km/sec [*Kieffer,* 1970]. Durations of shock pressures above 30 kb are estimated to be 10 to 45 msec [*Kieffer,* 1970].

STRUCTURE OF SHOCK FRONT IN GRANULAR QUARTZ

A theoretical one-dimensional model [*Kieffer,* 1968, 1970] was used to attempt to explain the fundamental mechanisms of energy deposition that occur as a shock passes through a granular material and to examine the effect of the porosity on these processes.

The geometry of the theoretical model is shown in Figure 14. An infinitely long quartz driver impacts one-dimensional grains separated by gaps. The Coconino sandstone shocked in the laboratory [*Ahrens and Gregson,* 1964; *Shipman and Gregson,* 1970] had a reported porosity of 25%; hence detailed calculations were done with this porosity so that the computed results could be compared with laboratory equation-of-

state data. The case of 25%-porosity, 0.2-mm-thick grains is shown in Figure 14. A similar model was used to study porous aluminum by *Hoffman et al.* [1968].

Finite difference analogs to the one-dimensional Lagrangian equations of conservation of mass, momentum, and energy are solved in conjunction with an appropriate equation of state for quartz. For this purpose, a computer program, purchased through Cosmic (Computer Software Management and Information Center) and originally developed by *Herrman et al.* [1967] at Sandia Corporation, was modified from a CDC 3600 computer to the IBM 360. The details of these calculations are given in *Kieffer* [1970].

Consider the sequence of events illustrated in Figure 14. As the driver, which is given an initial velocity v_0, hits the first plate, a shock is sent to the right in that plate and to the left in the driver. This shock takes the material to a state S_1 at pressure P_1 and compressed specific volume V_1. The right-traveling wave in the first grain reflects from the right free surface at the first pore as a rarefaction, or release, wave. The material is released to a state R_1 at lower pressure and greater specific volume than in the shock state. This rarefaction accelerates the free surface across the pore, and the rarefaction travels back through the first grain reducing

the pressure gradually to low values. After the grain has traversed the pore, it impacts the second grain. This again sends shock waves to the right and to the left from the interface, shock state S_2. Because of the increase of wave velocity with pressure, a trailing wave will overtake a leading wave. Hence, the left-traveling shock generated by the second impact will travel back through the first grain, overtaking the first rarefaction, which was, in turn, overtaking the first left-traveling shock. This process is repeated over and over as successive grains impact and waves are sent back into previously shocked material. It is this process of reverberation of shock and rarefaction waves through the grain that results in the deposition of energy in a porous material in excess of that deposited in a solid material of the same mineral composition.

Figure 15 is a pressure-specific volume diagram of the thermodynamic paths that a unit mass of material (shown in Figure 14 in grain number 1) follows to a final steady state for cases of three different porosities. The initial conditions appropriate to this graph are an impacting driver velocity of 1.5 km/sec, porosities of 5%, 25%, and 35%, and 0.20-mm quartz grains. Consider the middle figure for the case of 25% porosity. The upper dots represent shock states (numbered in succession), and the lower x's are the corresponding release states as the respective shocks are reflected from free surfaces adjacent to pores, and correspond to the states S_1, S_2, $\cdots$ and R_1, R_2, $\cdots$ described above. Final equilibration occurs to a pressure of 63 kb, specific volume 0.3407 g/cm^3. The equilibration pressure is taken as the average of the last computed shock and rarefaction pressure. Later rarefactions from the back of a driver of finite length (or from the edges of a meteorite) would reduce this equilibration pressure to zero.

This model can be expected to give a reasonable approximation to the shock history of real Coconino sandstone grains only at those pressures where pore space is totally collapsed, but significant amounts of phase transitions have not occurred. Data published by *Shipman and Gregson* [1970] and *Ahrens and Gregson* [1964] suggest that this range is between 55 and 130 kb. The equilibrium point calculated at 63 kb by this one-dimensional model falls within the scatter of measured sandstone Hugoniot data
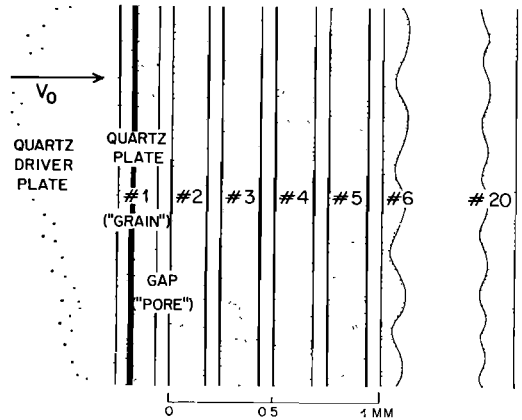

Fig. 14. Geometry of one-dimensional impact, showing plates separated by pores and driver plate, which is assumed to be infinitely long. Shock history of unit mass of material in grain 1 is considered in text.

and very close to (P, V) points at 67 kb, 0.330 cm^3/g, measured by Ahrens and Gregson, and 66 ± 1 kb, 0.341 ± 0.003 cm^3/g, measured by Shipman and Gregson (Figure 16). For purposes of comparison, Figure 15 illustrates the difference in final state in material of three porosities produced by the same driver impacting velocity.

For a given grain size, the length of time until equilibration occurs is governed by the porosity. The length of time to reach an oscillation of $1/e$ of the peak pressure varies from a few tenths of a microsecond for the case of 5% porosity to several microseconds for 35% porosity. This corresponds to the passage of the shock through four grains in a 5% porosity material and through more than 15 grains of 35% porosity. These equilibration times are appropriate to the one-dimensional model and can only describe qualitatively the rate of approach to equilibrium.

It is not directly predictable from a macroscopic model of the shock process that the peak pressure (105 kb in the sample case of 25% porosity shown in Figure 15) seen by individual grains in a porous material is much greater than the final equilibration pressure (63 kb). It has been hypothesized [*Shipman and Gregson*, 1970] that phase transitions in porous media proceed at lower (equilibration) pressures than in solid material because porous material is hotter under shock conditions. This model
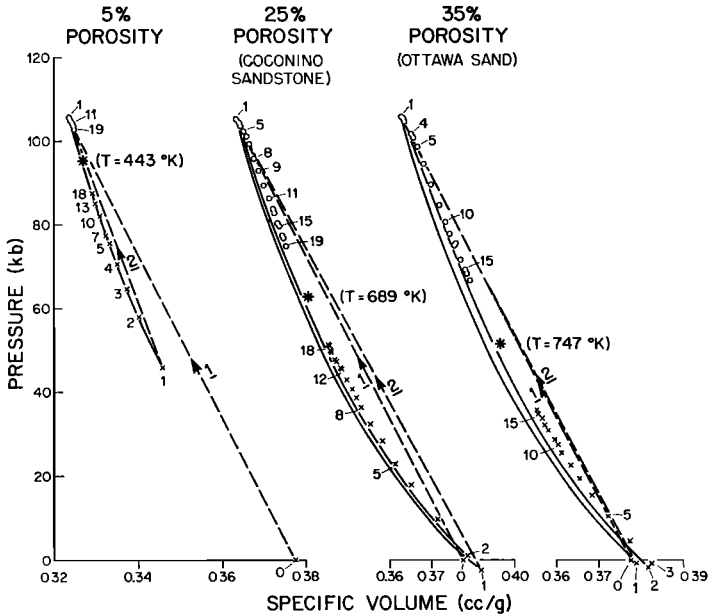
Fig. 15. Pressure-specific volume diagram of thermodynamic paths of unit mass of material in grain 1. The history of a grain within media of three different porosities is shown. Successive shock states are indicated by circles, successive release states by ×'s and are numbered according to the number of shocks that have passed through the material. Two successive Rayleigh lines are indicated by dashed lines; successive release adiabats are solid curves. Final equilibration states are indicated by an asterisk and are taken to be the average pressure and volume of the last computed shock states and rarefaction states.

suggests an additional reason why the phase changes appear to proceed at lower final equilibration pressures; peak shock pressures in the grains may be comparable to single-crystal transition pressures, even though the final equilibration pressure is less, and significant residence time may be spent at the higher pressures. 'Points' and irregularities in geometry in real sand grains may create spots of even locally greater pressure than predicted by the one-dimensional model.

With the use of this model, the effect of nonuniform porosity, due either to bedding or to local variations in porosity, was examined. Regions of locally varying porosity in the original material affect the shock and cause relatively hotter and cooler spots to form as the shock wave passes. The 'hot spots' are the focus of energy deposition and might be expected to contain areas of more highly metamorphosed grains. A few specific cases of variable porosity were examined. Because of the multitude of variations in porosity that could exist in a sandstone, local temperature increases of 100°

seem plausible because of this mechanism (at peak pressures of 100 to 200 kb).

Variations of initial porosity may cause variations of deposition of energy over a distance of several grain widths. To explain the observed relationships of fracturing and high-pressure phases in the shocked Coconino, however, a mechanism is required that will allow deposition of energy locally at the grain boundaries. This mechanism does not appear to be available in the one-dimensional model [Kieffer, 1970].

The conclusions from the one-dimensional consideration of energy deposition in a porous material may be summarized as follows:

1. The mechanism of equilibration to a final thermodynamic state in a granular material is the reverberation of shock and rarefaction waves created by multiple grain impacts.

2. The reverberation results in the deposition of energy in a porous material in excess of that deposited in a similar solid material because there are differences in the thermodynamic paths for each successive wave.

3. Peak shock pressures in individual grains

may be as much as twice the final steady-state pressure. In the case of quartz, the grain may have significant residence time in a stability field other than that to which it finally equilibrates.

4. Local variations of porosity within a material before it is shocked may account for nonuniform deposition of energy in grains.

5. The reverberation of shock and rarefaction waves can account for the average shock properties of a granular material (P, V, T) but cannot account for the microscopically observed nonuniformity of energy deposition.

6. Large dynamic viscosity at grain boundaries may be a cause of local energy deposition, but real viscosities appear to be too small to account for local energy deposition.

EXPERIMENTAL DATA ON SHOCKED COCONINO SANDSTONE

One of the goals of this study of the Coconino sandstone is to correlate petrographic properties of a naturally shocked rock with shock behavior measured in laboratory experiments on specimens of the same rock shocked to known pressures. Previous studies of shocked rocks have relied on experimental Hugoniot data for single crystals (e.g., quartz, feldspar, biotite) to
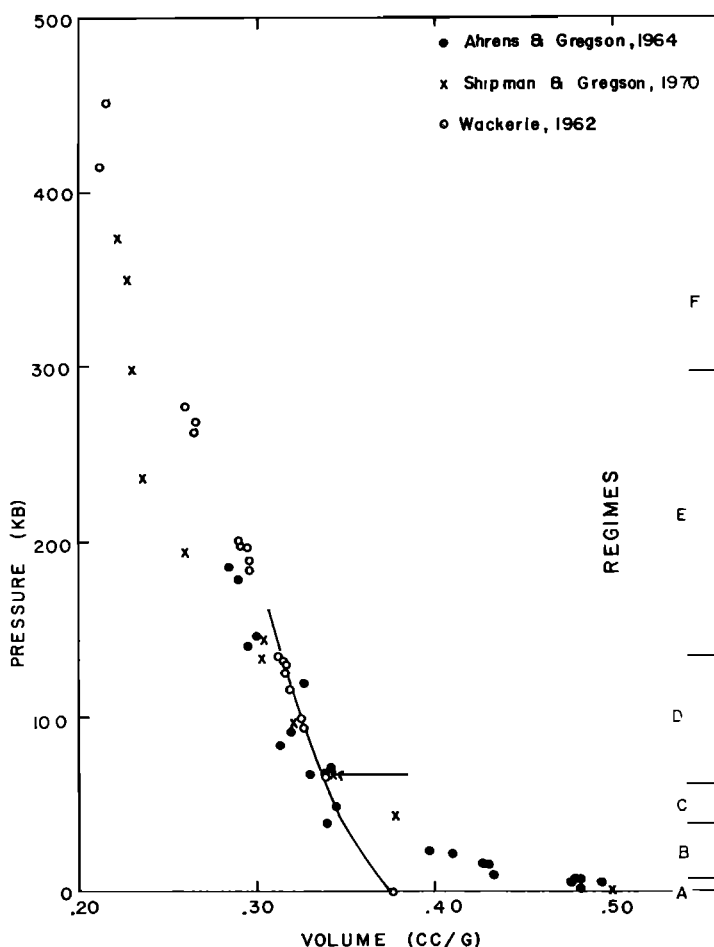

Fig. 16. Measured Hugoniot data points for Coconino sandstone ($\times$, $\bullet$) and single crystal quartz ($\circ$). The solid line is the Murnaghan equation for single-crystal quartz used in the one-dimensional model. The tip of the arrow represents a shock state computed by the one-dimensional model. Regimes of the Hugoniot described in Table 2 are indicated on the right ordinate.

estimate pressures and temperatures in the rocks [*Chao*, 1968; *von Engelhardt and Stöffler*, 1968]. These previous studies and the observations on naturally shocked Coconino demonstrate that nonuniform conditions of pressure and temperature occur at least temporarily in rocks. However, pressure equilibration, if not thermal equilibrium, is probably attained in the rock within the first few microseconds after the passage of the leading edge of the shock, and it is desirable to have some estimate of this equilibration pressure. With a careful interpretation of the Coconino sandstone equation-of-state data and observations of shocked sandstone, estimates of this pressure can be made for the Meteor Crater rocks.

Experimental data on shocked Coconino sandstone has been reviewed by *Kieffer* [1970]. The most important effects of shock metamorphism, the transitions to high-pressure phases, may be time dependent. The quartz-coesite transition is sluggish under conditions of static compression experiments [*Boyd and England*, 1960; *MacDonald*, 1956; *Griggs and Kennedy*, 1956; *Kitahara and Kennedy*, 1964] and shock experiments [*Chao et al.*, 1960; *DeCarli and Jamieson*, 1959]. The reaction rate is accelerated by the presence of shear stresses [*Bell and Boyd*, 1968]. Stishovite or a short-range order form of SiO_2 with Si in sixfold coordination, can apparently form in shock waves of microseconds' duration [*DeCarli and Milton*, 1965; *Ahrens and Rosenberg*, 1968].

A system of pressure regimes in which certain phenomena occur may be established for the Coconino sandstone from equation-of-state data [*Wackerle*, 1962; *Ahrens and Gregson*, 1964; *Shipman and Gregson*, 1970]. These regimes, used later in assigning pressures to the Meteor Crater rocks, are listed in Table 2 and shown in Figure 16.

SHOCK COMPRESSION OF THE COCONINO SANDSTONE

Interpretation of class 1 rocks. The porosity of class 1a rocks was slightly reduced by rotation of individual grains or groups of grains into the pores. Sufficient stresses passed through these rocks to break them loose from the bedrock and eject them from the crater. Because these rocks retain only slight permanent deformation, they were probably formed in regime A of the Hugoniot and have been shocked to equilibration pressures less than the 2–9 kb elastic limit measured by *Ahrens and Gregson* [1964]. Since almost no fracturing of grains occurred, peak pressures were probably less than 10 kb.

At slightly higher pressures, characteristic of class 1b rock, grains were deformed by fracture, and small amounts of plastic deformation occurred. Concussion fractures due to tensile stresses in the initial moments of impact are observed radiating into the grains from the contact surface. The observed alignment of concussion axis directions may be interpreted to give the direction of shock passage. Nests of chips beside the contact surface and chips within the radial fractures and on the contact surface may be derived from the region of first contact.

The tensile strength of quartz is of the order of 1 kb [*Borg et al.*, 1960]. Maximum compressive stresses of 3 to 4 kb are sufficient to produce these fracture patterns if the grains are unconfined. The Hugoniot data indicate that pressures up to 55 kb (regime B) may be required to eliminate porosity during shock compression. Equilibration pressure in regimes B and C appear to produce no phase changes in laboratory-shocked rocks and may have existed in the class 1b rocks.

Interpretation of class 2 rocks. Pore closure and elimination of porosity in class 2 rocks were accomplished by a very different process than occurred in class 1 rocks. The grains appear to have flowed plastically around each other and into the pores, forming an intricate network that resembles a jigsaw puzzle.

The shape and distribution of the elongated and aligned symplektic regions in class 2 rocks suggest that they are associated with collapsed pores. Microcrystalline coesite formed in the symplektic regions and occurs only in rocks that have deformed plastically. Coesite occurs in class 2 rocks in regions where high local mean stresses and high shear stresses are believed to have been generated, that is, at the contact surface between irregularly shaped grains or on shear planes within the grains. Initial shear in a region may be necessary for the formation of coesite by shock. Microcrystalline coesite is believed to form slowly and under nonequilibrium conditions during the shock because:

1. The pressures required to produce the observed plastic yielding (35 kb to 130 kb) in coesite-bearing rocks probably are equal to or exceed the pressure required to produce coesite under hydrostatic conditions (30 to 100 or 120 kb); however, very little coesite is observed in these rocks and the coesite that does occur is located in regions believed subjected to high peak and shear stresses.

2. In the sequence of 48 shocked rocks studied, there is no rock that is composed entirely of coesite, which would be expected if coesite were formed rapidly in the shock front (and were not destroyed by high temperatures).

The replacement of quartz by coesite in vermicular habit appears in thin section to have proceeded more completely at the centers of the symplektic regions than in the extremities. The growth of coesite in regions away from the boundary regions of high stress and high initial internal energy may have been controlled by the temperature gradient from the boundary of the grain, which was initially the focus of energy deposition, into the center of the grain.

Peak pressures must have been greater than required for plastic yielding; values of 35 kb to 130 kb are suggested for the yield point. Peak pressures were probably less than 300

kb, the pressure at which single-crystal quartz appears to be completely converted to a high-pressure phase within microseconds. Class 2 rocks were probably formed at equilibration pressures appropriate to regime D, 55 to 130 kb.

Interpretation of class 3 rocks. Pore closure and grain deformation in the class 3 rocks were accomplished by plastic flow of the quartz grains. The cryptocrystalline coesite cores are believed to have been the regions of highest transient pressure. Since stishovite is found in the opaque regions adjacent to the cryptocrystalline cores, the minimum pressure in the cores must have exceeded 70 kb, the minimum pressure at which stishovite can form. Peak pressures may have been substantially higher.

The cryptocrystalline coesite cores were formed before the microcrystalline coesite found on their boundaries. The cryptocrystalline fabric of the coesite cores suggests that all quartz in the region was destroyed prior to nucleation of the cryptocrystalline coesite. Pressures near 250 to 300 kb are required to transform most of a quartz region to high-pressure phases by a single shock [*Ahrens and Rosenberg*, 1968]. At these pressures quartz is converted to stishovite or to a short-range-order glass in sixfold coordination. It is interpreted that the regions that now contain cryptocrystal-

TABLE 2. Regimes of the Coconino Sandstone Hugoniot

Regime	Pressure Range*	Phenomena/Interpretation
A	0 to 2–9 kb†	Elastic deformation. Very little grain damage.
B	2–9 to 30 kb (22–45 kb)	Volume of compressed sandstone greater than the zero-pressure volume of quartz, 0.377 cm³/g. Pores are present in the compressed state.
C	30 kb to 55 kb (36–130 kb)	Volume of compressed sandstone less than initial volume of quartz and approaches the volume of shocked single-crystal quartz at higher pressures. Porosity is reduced to zero.
D	55 kb to 130 kb	Sandstone Hugoniot follows closely single-crystal quartz Hugoniot. Possible formation of small amounts of coesite.
E	130 to 300 kb	Volume of shocked sandstone less than volume of shocked quartz. Release adiabat data indicate that high-pressure phases are present in single-crystal quartz shocked to these pressures.
F	>300 kb	Compressed density is appropriate to shocked stishovite. Release adiabats of single-crystal quartz suggest that quartz grains shocked above 350 kb melt to fused silica on release.

* Possible extreme values for upper limits as interpreted by *Ahrens and Gregson* [1964] and *Shipman and Gregson* [1970] are given in parentheses.

† These pressures are 'equilibration pressures', as the term was used in the discussion of the one-dimensional model. Peak pressures in individual quartz grains will be significantly greater, so phenomena of interest that may occur in individual quartz grains in the Coconino are listed in the adjacent column and are based on the data of *Ahrens and Rosenberg* [1968].

line coesite were temporarily shocked to pressures near 300 kb and that all the quartz in the core region was converted to stishovite or to a glass with Si in sixfold coordination. Owing to the decrease in entropy in conversion of quartz to the high-pressure phase, these regions became hot. Temperature gradients from $2°/\mu$ to $10°/\mu$ may have existed between these core regions and adjacent quartz [Kieffer, 1970]. (The temperature gradient depends on the pressure at which quartz is converted to stishovite, being higher at higher pressures.) Local peak pressures sufficient to form stishovite were maintained for only a few microseconds, and during this time radiation and conduction could not appreciably decrease the temperature gradient across the regions.

Release of locally high pressure occurred in a few microseconds (pressure disturbances are propagated with the local sound speed (3–10 mm/μsec) and therefore traverse a grain diameter in a fraction of a microsecond). As hot stishovite regions were released to pressures appropriate to coesite stability conditions, they inverted to form the coesite cores. The high temperature of the stishovite regions may have allowed the transition from stishovite to coesite to proceed instantaneously at the phase boundary, approximately 100–120 kb. If the inversion to coesite occurred at the phase boundary, the temperature decrease associated with the (endothermic) reaction may be estimated from the slope of the phase line and an assumed specific heat and is on the order of 100°. With this temperature decrease, the residual temperature of the cores may have been reduced to approximately the same temperature as the surrounding regions, or the cores may have remained several hundred degrees hotter than the surroundings, depending on the initial pressure at which stishovite was formed. If the cores were several hundred degrees hotter, heat would have been conducted from a hot core into the surroundings during the 25–30 msec before release occurred to pressures below 30 kb. It is possible then that heat flow from a residual hot core could have accelerated the rate of formation of coesite in the adjacent opaque and symplektic regions by increasing the temperature of the region.

In those coesite-rich regions that do not contain cores, a temperature gradient from regions of initial stress concentrations into the grain interiors may have controlled the rate of growth of coesite from quartz. Further discussion of temperature gradients in these rocks is given in Kieffer [1970].

Metastable stishovite was preserved as the rarefaction wave released material through the coesite and quartz stability fields only in those regions that were relatively cool, that is, in the opaque material exterior to the main region of stishovite formation; most of the stishovite that was formed inverted to cryptocrystalline coesite. Approximately half of the coesite in some of these rocks is in the cryptocrystalline cores and is assumed to have been formed by the inversion of stishovite (or a glass with Si in sixfold coordination). Large amounts of metastable coesite are preserved apparently because of slow reaction rates at the low temperatures in the material by the time it is released to 30 kb.

The sequence of events for characteristic class 3 rocks is interpreted to have been as follows. On impact of grains across pores, stishovite was formed from metastable quartz at pressures estimated to have been in excess of 250 kb. The temperature of these cores depended on the pressure at which they were formed, but temperature gradients of $10°/\mu$ appear likely for cores formed at pressures in excess of 250 kb. On release of the locally high pressure in the stishovite region, coesite nucleated at many random sites, forming cryptocrystalline cores and lowering the excess temperature of the core region by about 100°C. Microcrystalline coesite nucleated from quartz adjacent to the core regions. Heat conducted outward from the hot core into the surroundings may have accelerated the transformation rate of the quartz-coesite reaction, causing abundant coesite to form in these rocks during the release of the material through the coesite stability field. The formation of coesite may have stopped when transient high temperatures decreased below certain levels or may have continued, at a decreasing rate, until the pressure decayed below 30 kb. Small amounts of stishovite are preserved in opaque regions, which are interpreted to have been relatively cool regions. The phases were then preserved metastably by quenching as the temperature decreased.

Pressures greater than 250–300 kb at grain boundaries probably did not exist for more than a few microseconds. Final equilibration pressures must have been less than 250 kb to account for the amount of residual quartz in the rocks. Peak pressures at grain boundaries were probably less than 350 kb, the pressure at which stishovite inverts to fused silica on release to low pressures.

Interpretation of class 4 and class 5 rocks. Class 4 rocks are characterized by large areas of vesicular glass adjacent to coesite-rimmed quartz grains. Class 5 rocks are, for the purpose of this discussion, considered to be products of the processes described below in the limit of very high pressure.

The occurrence of vesicular glass in cores similar to the cryptocrystalline coesite cores of class 3 rocks suggests that the glass was formed from the same initial material as the cryptocrystalline coesite. These regions were apparently composed of stishovite or dense glass formed above 350 kb. On release from pressures above this value, stishovite inverts to glass [*Ahrens and Rosenberg*, 1968], which is the material seen at present in the cores.

Skinner and Fahey [1963] first suggested that all the silica glass found in direct association with stishovite formed by the breakdown of stishovite. Although measurements of amounts of phases in the shocked Coconino show that there is little glass in rocks containing detectable stishovite (class 3), the spatial relationships between the quartz, coesite, and glass in class 4 rocks suggests that the lechatelierite in these nonstishovite-bearing rocks formed by inversion of stishovite on release to low pressures. Coesite may have been formed as an intermediate phase and then inverted to the observed glass. In contrast, *Stöffler* [1971] and *von Engelhardt and Bertsch* [1969] believe that stishovite in the crystalline Ries rocks inverts to diaplectic glass, not lechatelierite. It must be kept in mind that at comparable equilibration pressure, shocked Coconino sandstone will have experienced a very different (and hotter) thermodynamic history than the crystalline rocks. There is, therefore, no a priori reason to believe that the processes of phase changes in SiO$_2$ are similar in the two instances.

In class 4 and 5 class 5 rocks, coesite that was adjacent to the stishovite cores apparently in-

verted to glass because of high residual temperatures; it is preserved only as rims against quartz grains, which must have been the regions that remained at lowest temperature during shock compression of the class 4 and class 5 rocks. The relatively large abundance of coesite in class 4 rocks containing 30 to 40% quartz and no stishovite is compatible with observations that coesite is the more stable metastable phase at ambient pressure [*Dachille et al.*, 1963; *Gigl and Dachille*, 1968; *Skinner and Fahey*, 1963].

REFERENCES

Ahrens, T. J., and V. G. Gregson, Jr., Shock compression of crustal rocks: Data for quartz, calcite, and plagioclase rocks, *J. Geophys. Res., 69,* 4839–4874, 1964.

Ahrens, T. J., and J. T. Rosenberg, Shock metamorphism: Experiments on quartz and plagioclase, in *Shock Metamorphism of Natural Materials,* edited by B. French and N. Short, Mono, Baltimore, Md., 1968.

Akimoto, Syun-Iti, and Yasuhito Syono, Coesite-stishovite transition, *J. Geophys. Res., 74,* 1653, 1969.

Barringer, D. M., Coon Mountain and its crater, *Proc. Nat. Acad. Sci., Philadelphia, 57,* 861–886, 1905.

Barringer, D. M., *Meteor Crater (formerly called Coon Mountain or Coon Butte) in Northern Central Arizona,* 24 pp., published by the author, 1909.

Bell, P. M., and F. R. Boyd, Phase equilibrium data bearing on the pressure and temperature

of shock metamorphism, in *Shock Metamorphism of Natural Materials,* edited by B. French and N. Short, Mono, Baltimore, Md., 1968.

Bjork, R. L., Analysis of the formation of Meteor Crater, Arizona, *J. Geophys. Res., 66,* 3379–3387, 1961.

Borg, I., M. Friedman, J. Handen, and D. V. Higgs, *Experimental Deformation of St. Peter Sand: A Study of Cataclastic Flow, Mem. 79,* p. 133, Geological Society of America, Boulder, Colo., 1960.

Boyd, F. R., and J. L. England, The quartz-coesite transition, *J. Geophys. Res., 65,* 749, 1960.

Boyd, F. R., P. M. Bell, J. L. England, and M. C. Gilbert, Pressure measurement in single-stage apparatus, *Carnegie Inst. Wash. Yr. Book, 65,* 410, 1966.

Bunch, T. E., and A. J. Cohen, Shock deformation of quartz from two meteorite craters, *Bull. Geol. Soc. Amer., 75,* 1263, 1964.

Carter, N., Dynamic deformation of quartz, in *Shock Metamorphism of Natural Materials,* edited by B. French and N. Short, Mono, Baltimore, Md., 1968.

Chao, E. C. T., Impact metamorphism, in *Researches in Geochemistry,* vol. 2, John Wiley, New York, 1967.

Chao, E. C. T., Pressure and temperature histories of impact metamorphosed rocks—based on petrographic observations, in *Shock Metamorphism of Natural Materials,* edited by B. French and N. Short, p. 149, Mono, Baltimore, Md., 1968.

Chao, E. C. T., E. M. Shoemaker, and B. M. Madsen, First natural occurrence of coesite, *Science, 132,* 220, 1960.

Chao, E. C. T., J. J. Fahey, and J. Littler, Stishovite, SiO₂, a very high pressure new mineral from Meteor Crater, Arizona, *J. Geophys. Res., 67,* 419, 1962.

Coes, L., Jr., A new dense crystalline silica, *Science, 118,* 131–133, 1953.

Cohen, Lewis H., and William Klement, Jr., High-low quartz inversion: Determination to 35 kilobars, *J. Geophys. Res., 72,* 4245, 1967.

Dachille, F., and R. Roy, High-pressure region of the silica isotopes, *Z. Krist., 111,* 451, 1959.

Dachille, F., R. J. Zeto, and R. Roy, Coesite and stishovite: Stepwise reversal transformations, *Science, 140,* 991, 1963.

DeCarli, P. S., and J. C. Jamieson, Formation of an amorphous form of quartz under shock conditions, *J. Chem. Phys., 31,* 1675–1676, 1959.

DeCarli, P. S., and D. J. Milton, Stishovite: Synthesis by shock wave, *Science, 147,* 144–145, 1965.

Fairchild, H. L., Origin of Meteor Crater (Coon Butte), Arizona, *Bull. Geol. Soc. Amer., 18,* 493–504, 1907.

French, B., and N. Short, Eds., *Shock Metamorphism of Natural Materials,* Mono, Baltimore, Md., 1968.

Gigl, P. D., and F. Dachille, Effects of pressure and temperature on the reversal transitions of stishovite, *Meteoritics, 4,* 123–136, 1968.

Griggs, D. T., and G. C. Kennedy, A simple apparatus for high pressures and temperatures, *Amer. J. Sci., 254,* 722, 1956.

Herrmann, W., P. Holzhauser, and R. J. Thompson, WONDY, A computer program for calculating problems of motion in one dimension, *Sandia Res. Rep. SC-RR-66-601,* Albuquerque, New Mexico, 1967.

Hertz, H., On the contact of elastic solids, in *Miscellaneous Papers,* Chap. 5, translated by D. E. Jones and G. H. Schott, Macmillan, London, 1896.

Holm, J. L., O. J. Kleppa, and E. F. Westrum, Thermodynamics of polymorphic transformations in silica: Thermal properties from 5 to 1070°K and pressure-temperature stability fields for coesite and stishovite, *Geochim. Cosmochim. Acta, 31,* 2289, 1967.

Hoffman, R., D. J. Andrews, and D. E. Maxwell, Computed shock response porous aluminum, *J. Appl. Physics, 39,* 4555, 1968.

Hörz, F., Statistical measurements of deformation structures and refractive indices in experimentally shock-loaded quartz, in *Shock Metamorphism of Natural Materials,* edited by B. French and N. Short, Mono, Baltimore, Md., 1968.

Kennedy, G. C., G. J. Wasserburg, H. C. Heard, and R. C. Newton, The upper three-phase region in the system SiO₂-H₂O, *Amer. J. Sci., 260,* 501, 1962.

Kieffer, S. W., Shock wave propagation through granular quartz, *Eos, Trans. AGU, 50,* 221, 1968.

Kieffer, S. W., 1, Shock metamorphism of the Coconino Sandstone at Meteor Crater, Arizona; 2, The specific heat of solids of geophysical interest, Ph.D. thesis, California Institute of Technology, Pasadena, 1970.

Kitahara, S., and G. C. Kennedy, The quartz-coesite transition, *J. Geophys. Res., 69,* 5395, 1964.

MacDonald, G. J. F., Quartz-coesite stability relations at high temperatures and pressures, *Amer. J. Sci., 254,* 713, 1956.

McKee, E. D., The Coconino sandstone—its history and origin, *Carnegie Inst. Wash. Pap. Concerning Palaeontol. Calif., Ariz., Idaho, Publ. 440,* p. 79, March 1934.

Merrill, G. P., and W. Tassin, Contributions to the study of the Canyon Diablo meteorites, *Smithson. Misc. Collections, 50,* pp. 203–215, 1907.

Merrill, G. P., On a peculiar form of metamorphism in siliceous sandstone, *Proc. U.S. Nat. Museum, 32,* 547, 1908.

Ostrovsky, J. A., Experimental fixation of the position of the coesite-stishovite equilibrium curve (in Russian), *Izv. Akad. Nauk SSSR Ser. Geol.,* no. 10, 132, 1965.

Ostrovsky, J. A., On some sources of errors in phase-equilibria investigations at ultra-high pressure, *Geol. J., 5,* 321, 1967.

Rogers, A. F., Natural history of the silica minerals, *Amer. Mineral., 13,* 73–92, 1928.

Shipman, F. H., and V. G. Gregson, *A Shock Wave Study of Coconino Sandstone, Final Rep.,* part 1, Materials and Structures Lab., General Motors Corp., Warren, Michigan, 1970.

Shoemaker, E. M., Penetration mechanics of high-velocity meteorites, illustrated by Meteor Crater, Arizona, *Rep. Int. Geol. Congr., 21st Sess., Norden, Germany, 18,* 418, 1960.

Shoemaker, E. M., Impact mechanics at Meteor Crater, Arizona, in *The Solar System,* vol. 4, *The Moon, Meteorites and Comets,* edited by B. M. Middlehurst and G. P. Kuiper, p. 301, University of Chicago Press, 1963.

Skinner, B. J., and J. J. Fahey, Observations on the inversion of stishovite to silica glass, *J. Geophys. Res., 68,* 5595, 1963.

Stishov, S. M., On the equilibrium line between coesite and rutile-like modification of silica (in Russian), *Dokl. Akad. Nauk SSSR, 148*(5) 1186, 1963.

Stöffler, D., Coesite and stishovite in shocked crystalline rocks, *J. Geophys. Res., 76,* this issue, 1971.

Takahashi, T., Factors influencing pressure in multi-anvil devices, in *High-Pressure Measurement,* edited by A. A. Giardini and E. C. Lloyd, p. 240, Butterworth, Washington, D.C., 1963.

Tilghman, B. C., Coon Butte, Arizona, *Proc. Acad. Nat. Sci. Philadelphia, 57,* 887–914, 1905.

Timoshenko, S., and J. N. Goodier, *Theory of Elasticity,* 3rd ed., McGraw-Hill, New York, 1970.

von Engelhardt, W., and W. Bertsch, Shock-induced planar deformation structures in quartz from the Ries crater, Germany, *Contr. Mineral. Petrol., 20,* 203, 1969.

von Engelhardt, W., and D. Stöffler, Stages of shock metamorphism in crystalline rocks of the Ries basin, Germany, in *Shock Metamorphism of Natural Materials,* edited by B. French and N. Short, Mono, Baltimore, Md., 1968.

von Engelhardt, W., J. Arndt, D. Stöffler, W. F. Müller, H. Jeziorkowski and R. A. Gubser, Diaplektische Gläser in den Breccien des Ries von Nördlingen als Anzuchen für Stossvellenmetamorphose, *Contrib. Mineral. Petrol., 15,* 93–102, 1967.

Wackerle, J., Shock-wave compression of quartz, *J. Appl. Phys., 33,* 922, 1962.